Revisiting the Effective SINR Mapping Interface for Link and System Level Simulations of Wireless Communication Systems

E. M. G. Stancanelli, F. R. P. Cavalcanti, Y. C. B. Silva
Federal University of Ceará (UFC)
Wireless Telecommunications Research Group (GTEL)
CP 6005, Campus do Pici, 60455-760, Fortaleza-CE, Brazil
{emiguel, rodrigo, yuri}@gtel.ufc.br

***Abstract*—Exponential effective signal-to-interference plus noise ratio mapping, also known as EESM, is a link-to-system level (L2S) interface that have been successful to exchange information between a system-level simulator (SLS) and a link-level simulator (LLS). However, in some special adverse conditions, such as where the Gaussian distribution does not hold for the interference term, the accuracy provided may not be suitable to radio resource management and link adaptation algorithms. If, on the one hand, the effective channel quality facilitates creating the lookup tables as well as mapping throughout them, on the other hand, it can erroneously lead SLS to obtain similar results for distinct physical-level states. This work addresses that issue and devises a workaround solution in order to visualize the potential benefits on overcoming this drawback. An extended version of EESM is introduced and, through computer simulations, its improvements are corroborated.**

***Index Terms*—Wireless Communication. Computer Simulation. Link-to-System level interface. Co-channel Interference.**

I. Introduction

The computer simulation method has been showing increasingly importance in assessing the performance of a cellular network, by making easier to isolate and track specific events [1]. Due to the richness of details involved in modeling such networks, in most cases the researchers have divided the simulator in two parts [2]: link-level simulator (LLS) and system-level simulator (SLS). While the LLS part evaluates the radio link operation by simulating the channel coding, modulation and radio channel propagation; the SLS part aims at reproducing the systemic characteristics of the network, including users' mobility, admission/blocking of connections, scheduling, radio resources allocation, and traffic generation.

Besides, a method for interfacing LLS and SLS must be accomplished as well, named link-to-system level (L2S) interface, enabling both good accuracy of results and computational feasibility. A number of publications deals with this matter, providing well-known solutions such as the average value interface (AVI), the actual value interface (AcVI) [3], [4], and the effective signal-to-interference plus noise ratio mapping (ESM) technique [5], [6]. In all of them, the aim is to avoid the need to run the LLS each time the SLS requires a prediction of the link-level performance. Instead the SLS will just consult a lookup table which stores statistics about the link-level performance. This is justified by saving of computational complexity.

In ESM solutions, the interface is built from instantaneous channel quality measures. The signal-to-interference plus noise ratio (SINR) is typical channel quality measure, in which any individual information concerning thermal noise or co-channel interference terms is discarded. Moreover, channel quality measure is a compressed information extracted from the multidimensional physical-level state.

Those summarizing operations may be harmful to the predictions taken by SLS on certain simulation conditions, which we refer to as adverse conditions. Scenarios contaminated by non-Gaussian distributed interference are a possible cause of adverse conditions. As an investigation of such adverse conditions, in this paper we focus on a cell-edge mobile user equipment (UE) in an orthogonal frequency division multiplexing (OFDM)-based downlink system in order to verify the inaccuracy of the ESM approach.

The remainder of this work is organized as follows. In section II we briefly present some peculiarities of the interference-limited scenarios of OFDM-based systems. In section III we review the classical exponential ESM (EESM) approach as the well-known ESM L2S interface. The inability of the classical EESM to deal with adverse conditions is addressed in section IV and, in addition, a simple solution is introduced. Finally, we describe an LLS employed to evaluate the L2S interface in section V, as well as we discuss the benefits of overcoming the drawback of the classical EESM.

II. Typical Interference-limited Scenarios

Consider a Long Term Evolution (LTE) OFDM-based downlink [7] and assume that the orthogonality among the subcarriers is preserved and there is no other system using the same radio resources. A number of base stations (BSs) are present in the system, which we can classify as serving base station (sBS) – those BSs supposed to transmit to a given UE – and interfering base station (iBS) – the other ones.

Consider a group of nineteen three-sectorized cells uniformly spaced, as illustrated in Fig. 1. A full frequency reuse scheme is employed. Without loss of generality, BS 4 plays the role of sBS.

978-1-4673-0279-1/11/$26.00 ©2011 IEEE

The UE receiver antenna is assumed to be omni-directional, whereas all involved transmission antennas are assumed to be directional for a 120° sector, with the radiation pattern in the horizontal plane given in accordance with [8], in dB:

$$G^{(a)}(\theta) = -\min\left\{12\left(\frac{18}{7\pi}\theta\right)^2, 20\right\} + 14, \quad (1)$$

where θ is the azimuth in radians.

All the BSs are transmitting with the same power and are subjected to the same path loss, such as the average $G^{(\mathrm{pl})}_{j,m}(d)$, in dB, for a UE j distant d meters from BS m, according to simulation case 1 of [9],

$$G^{(\mathrm{pl})}_{j,m}(d) = 35.3 + 37.6\log_{10}(d). \quad (2)$$

In Fig. 1, the sectors belonging to BSs from 1 to 3 and from 5 to 7 constitute the first-interfering-ring, whereas the second-interfering-ring sectors are those belonging to BSs from 8 to 19. Let us assume that the sectors of each cell are numbered from one to three, beginning from the bottom one and increasing clockwise.

We have simulated a single UE moving over the first sector of sBS (see Fig. 2), going from the sBS-site (cell-center) — marked as ♦ — straight ahead to the most extreme edge point (cell-edge) — marked as ●. The cell radius R is of 334 m.

During the journey of this UE, we recorded the received signal strength from each participating BS. In Fig. 3, we show these signal strength levels for the most significant iBSs, normalized at each UE position by the strength of the signal from the sBS's first sector. While the UE stays in the cell-center region – say a distance up to $0.25R$ from the sBS – we have not found any expressive interfering source – say a normalized interference signal level greater than -10 dB. As UE moves away from the center, the interfering signals tend to become more expressive, until, once in cell-edge region – say a distance at least $0.70R$ from the sBS – one expressive iBSs probably will be highlighted.

Thereafter we assume that the resultant interfering signal seen from the cell-edge UE receiver is composed by one or at most two dominant iBSs. This way, the central limit theorem cannot be straightforwardly applied here and, afterwards, to know how the UE demodulator will suffer the interference signal, the exact modulations used by all the involved BSs must be taken into account. As a consequence, the link-level answers differently whether the corruption of reception is due to thermal noise, co-channel interference or to both of them.

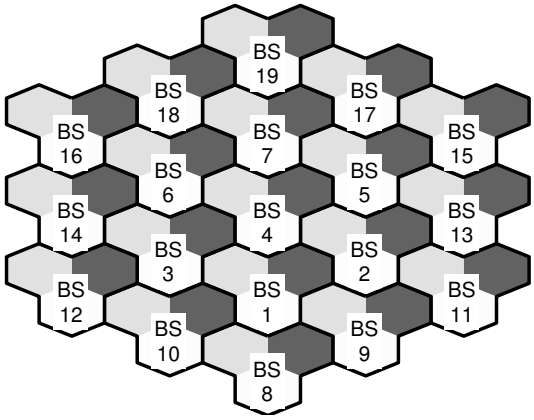

Fig. 1. Group of nineteen cells, with the BS 4 as the sBS, the BSs from 1 to 3 and from 5 to 7 constitute the first-interfering-ring, and the BSs from 8 to 19 the second-interfering-ring.

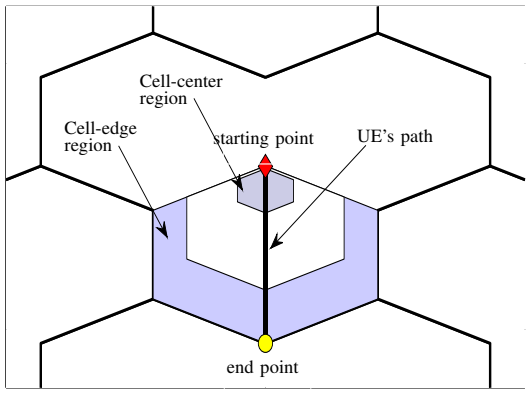

Fig. 2. A UE moving from the cell-center of sBS (viz. BS 4) to the cell-edge.

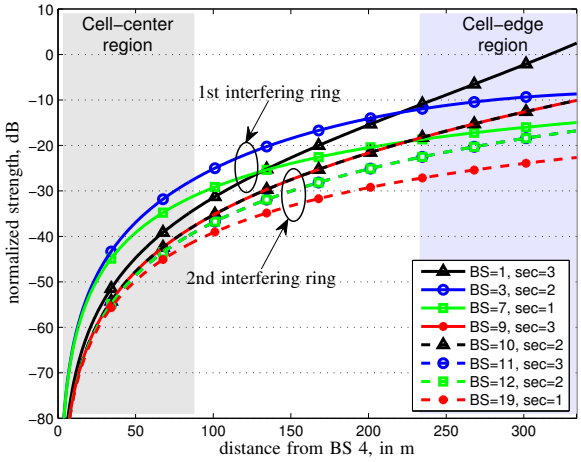

Fig. 3. Samples of the iBSs' normalized signal strengths taken along the path of a moving UE.

III. Effective SINR Mapping

ESM is a family of L2S interface approaches, in which an effective channel quality measure for a multidimensional channel is adopted. Moreover, unlike AVI and AcVI, ESM takes into account instantaneous channel conditions [5], which has turned it an attractive approach.

The ESM usually operates in a two-stage scheme. The first stage of ESM is called *SINR compression*, in which the dimensionality of channel quality measures is reduced as low as to one. Let γ_k be the SINR measure of the k-th subcarrier, the instantaneous channel state comprising all K assigned

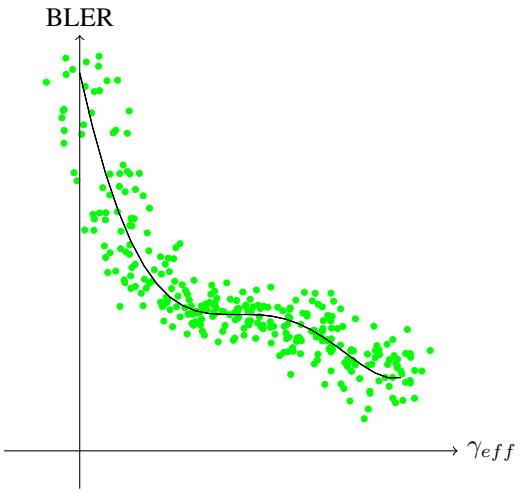

Fig. 4. The relationship provided by the classical EESM L2S between the γ_{eff} and $BLER$ measures and the quality mapping curve.

subcarriers will be represented by $\boldsymbol{\gamma} = \begin{bmatrix}\gamma_1 & \gamma_2 & \cdots & \gamma_K\end{bmatrix}^T$. The SINR compression stage yields the effective channel quality in terms of SINR, γ_{eff}.

In the EESM, herein named classical EESM, one of the main ESM versions, γ_{eff} is given by [5]:

$$\gamma_{eff} = -\alpha \ln\left(\frac{1}{K}\sum_{k=1}^{K}\exp\left(-\frac{\gamma_k}{\beta}\right)\right), \tag{3}$$

where α and β are the scaling factor parameters further used to calibrate the interface so as to reduce the mismatch between the actual and the predicted curves.

The second stage is the *quality mapping*, in which the effective channel quality is mapped to a given performance metric, such as bit error rate, packet error rate, block error rate (BLER) or throughput.

Fig. 4 depicts this, where each point in the scatter plot is a pair of γ_{eff} and $BLER$ obtained from LLS campaigns; then the curve represents the quality mapping to summarize such results in a plain way for the SLS.

The quality mapping function can be obtained from a regression over the set of data samples or alternatively the additive white Gaussian noise (AWGN) channel performance curve [5], [6], [10]. The proof for the latter, based on the Union Chernoff bound, can be seen in [10]. Yet the regression with Pth order polynomial over a dataset with N samples proceeds as follows.

Assume at each sample n, we know the effective SINR for a fixed value of the $\langle\alpha,\beta\rangle$ pair, $\gamma_{eff}(n)$, and the resulting BLER, $p(n)$. Then, we basically have to solve the system of linear equations:

$$\boldsymbol{p} = \boldsymbol{\Gamma}\boldsymbol{w}, \tag{4}$$

where

$$\boldsymbol{p} = \begin{bmatrix}p(1) & p(2) & \cdots & p(n) & \cdots & p(N)\end{bmatrix}^T, \tag{5}$$

$$\boldsymbol{w} = \begin{bmatrix}w_0 & w_1 & w_2 & \cdots & w_P\end{bmatrix}^T, \tag{6}$$

and

$$\boldsymbol{\Gamma} = \begin{bmatrix} 1 & \gamma_{eff}(1) & \gamma_{eff}(1)^2 & \cdots & \gamma_{eff}(1)^P \\ 1 & \gamma_{eff}(2) & \gamma_{eff}(2)^2 & \cdots & \gamma_{eff}(2)^P \\ & & \ddots & & \\ 1 & \gamma_{eff}(n) & \gamma_{eff}(n)^2 & \cdots & \gamma_{eff}(n)^P \\ & & & \ddots & \\ 1 & \gamma_{eff}(N) & \gamma_{eff}(N)^2 & \cdots & \gamma_{eff}(N)^P \end{bmatrix}. \tag{7}$$

The solution $\boldsymbol{w}^\star$ for $\boldsymbol{\Gamma}$ is known to be:

$$\boldsymbol{w}^\star = \boldsymbol{\Gamma}^T\left(\boldsymbol{\Gamma}\boldsymbol{\Gamma}^T\right)^{-1}\boldsymbol{p}. \tag{8}$$

Once $\boldsymbol{w}^\star$ is calculated, we will be able to directly estimate the BLER at a given instant n, $\widehat{p}(n)$, for any channel state, by calculating the $\gamma_{eff}(n)$ for a given $\langle\alpha,\beta\rangle$, and therefore

$$\widehat{p} = \begin{bmatrix}1 & \gamma_{eff} & \gamma_{eff}^2 & \cdots & \gamma_{eff}^P\end{bmatrix}\boldsymbol{w}^\star. \tag{9}$$

The configured interface can be evaluated by calculating the mean square error (MSE) over the estimates, $MSE_e = \frac{1}{N}\sum_n |p(n) - \widehat{p}(n)|^2$.

This procedure should be repeated for several $\langle\alpha,\beta\rangle$ pairs, choosing that pair whose MSE_e is the lowest; from this pair we will obtain the definitive $\boldsymbol{w}^\star$ and the interface will be calibrated. The calibration issue is addressed in [11]. Different pairs of parameter values will be associated to each modulation and coding scheme m, $\langle\alpha^\star;\beta^\star\rangle_m$.

IV. Extended EESM

The classical EESM is a very useful and reliable L2S interface as long as the interference is negligible or at least it presents a Gaussian probability density function. Otherwise, the SINR measure will not be an appropriate input of the compression stage, since different interfering scenarios with equal γ_{eff} may be confused with each other. In spite of different interfering scenarios tending to result in different BLER performance, this difference cannot be handled by the quality mapping stage.

Fig. 5 depicts the behavior of the classical EESM under an adverse condition, in which two possible interfering power levels are present. Note that while the γ_{eff} is the same, the resulting BLER can be different for each scenario. By following the procedure stated in section III, a single quality mapping curve will be given by $\boldsymbol{w}^\star$, and, therefore, probably an unreliable prediction will be provided to the SLS.

A plain solution can be obtained by tuning the EESM independently for each interference power level. For this purpose, we have to extract separately the interference-to-noise ratio (INR) and the signal-to-noise ratio (SNR) measures; the SINR measures are derived from them. In the sequel, we identify the most frequent interference power levels, obtaining a $\boldsymbol{w}^\star$ for each one. To this approach we refer as extended EESM. Fig. 6 illustrates an adverse condition characterized for two distinct interference power levels, each one must be detected by the SLS in order to be mapped on the appropriate curve.

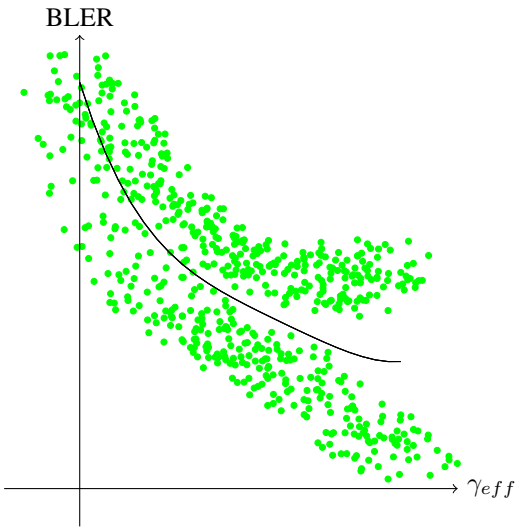

Fig. 5. The behavior of classical EESM under adverse condition, in which there are two different interfering levels; it provides an unreliable quality mapping.

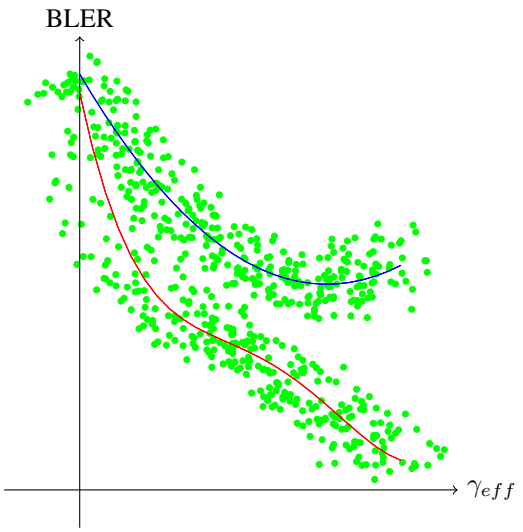

Fig. 6. The behavior of extended EESM under adverse condition, in which there are two different interfering levels; it provides two well-fitted quality mapping curves.

V. Computer Experiments

Through computer simulations, the ESM interface described in section III and its extended version described in section IV are evaluated and compared to each other herein. For this purpose, an LLS tool has been designed inspired on the 3rd. Generation Partnership Project (3GPP) LTE downlink features [7] and on some other ones described in the following.

Pursuing a scenario presenting adverse interfacing condition, we consider a single UE in the cell-edge region such that there is a received interfering signal whose average power has the same order of magnitude of the desired signal, say P_i and P_s respectively; we assume that the SLS is capable to perfectly discern these two parcels. Two independent BSs are modeled to transmit the desired and interfering signals.

This UE is simultaneously assigned to all available subcarriers, specifically $K = 256$ subcarriers spaced of $\Delta f = 15$ kHz with equal power allocation among them. The transmission chain comprises features as: 4 bits cyclic redundancy check; rate $1/3$ turbo coding with 13 and 15 as the feedback and feedforward generators in base-8, respectively; 8 bits guard period; and binary phase-shift keying modulation. The reception chain performs the reverse processing and mitigates the radio channel effects.

The UE is moving with a speed of 30 km/h, regarding both serving and interfering BSs, under the vehicular B channel model of International Telecommunication Union (ITU) [12], whose relative terms of the power-delay profile is shown in Table I.

TABLE I
ITU'S VEHICULAR B POWER-DELAY PROFILE.

delay (ns)	average power (dB)
0	-2.5
300	0.0
8 900	-12.8
12 900	-10.0
17 100	-25.2
20 000	-16.0

A channel realization comprises N consecutive transmission time intervals (TTIs), providing the channel quality measure $\boldsymbol{\gamma}_n$ and transmission outcome (success or failure) for each instant $n = 1, \ldots, N$. That same channel realization is repeated 500 times, while the random seeds of thermal noise and data traffic are reset to other values, so that an accurate estimate of BLER, p_n, can be obtained from the transmission outcomes. The pairs $\langle \boldsymbol{\gamma}_n, p_n \rangle$ will be taken as the common dataset for designing both L2S interfaces.

A. Results

In this section we show some simulation results for a scenario presenting adverse conditions for interfacing. Nevertheless we assume that we are able to discern how much the interference and thermal noise powers affect the radio link performance.

Let us define a scenario of adverse interfacing conditions as one in which P_i changes while the SINR has a fixed negative value of -3 dB. The average interference changing is modeled by switching, at each 20 000th TTIs, among three configurations: (i) initially there is no interference with $SNR = -3\ dB$ and $P_I = 0$; (ii) next both average power terms have the same participation, i.e., $SNR = 0\ dB$ and $P_I = P_S$; (iii) finally, the interference becomes highly dominant, by setting $SNR = 10\ dB$ and $P_I = 1.9 P_S$.

Fig. 7 is a plot of the series of p_n values observed during link-level simulations along with the three configurations above, for $n = 1, \ldots, 60\,000$.

For each configuration c, the first 10 000 time tags define the subset $\mathfrak{T}_c$; the next 5 000 time tags define the subset $\mathfrak{V}_c$; and the last 5 000 ones the subset $\mathfrak{L}_c$. By concatenating the datasets

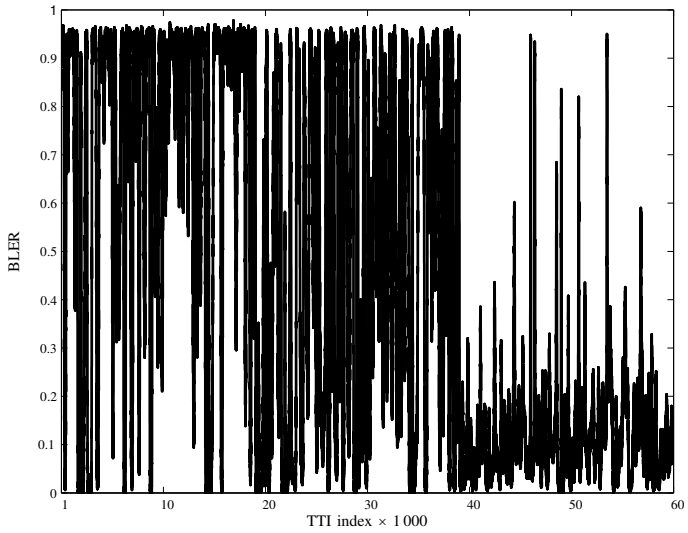

Fig. 7. Series of BLER values obtained from extensive link-level simulations.

of the three configurations, we define the time tag subsets used for configuring, validating (evaluation of configuring) and testing (evaluation after configuring is finished), respectively as $\mathfrak{T} = \bigcup_{c=1}^{3} \mathfrak{T}_c$, $\mathfrak{V} = \bigcup_{c=1}^{3} \mathfrak{V}_c$ and $\mathfrak{L} = \bigcup_{c=1}^{3} \mathfrak{L}_c$, as illustrated in Fig. 8. These subsets are equally used for designing both interfaces, when the procedures described in sections III and IV are rigorously followed.

Each EESM version was validated for several pairs $\langle \alpha, \beta \rangle$ and polynomial order P. We choose the combination of α, β and P that yields the lowest MSE. The lowest MSE values found for the classical and extended EESM are, 0.03975 and 0.01462, respectively.

Fig. 9(a) shows the actual p_n values provided by the LLS tool for a given testing subset. The responses provided by each L2S interface works as a prediction of such behavior, since this subset was not presented during configuring process. Fig. 9(c) and Fig. 9(c) show the results of prediction provided by the classical and extended EESM, respectively. Note that the prediction provided by the classical EESM cannot follow the changes on the interference configuration, but the extended EESM can.

MSE is not the most appropriate metric to solely analyze the L2S interface performance. The analysis over each individual sample of prediction (square) error seems to be a better strategy. In fact, by averaging the square errors, we lost the information whether that high MSE is due to several small square errors — or *weak fails* of the interface — or to a few large square errors — or *strong fails* of the interface. If each

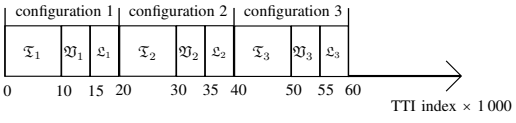

Fig. 8. The organization of the time tags into subsets for configuring, validating and testing of the classical and extended EESM interfaces.

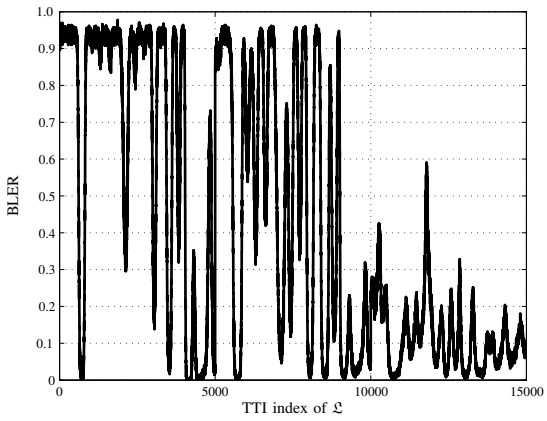

(a)

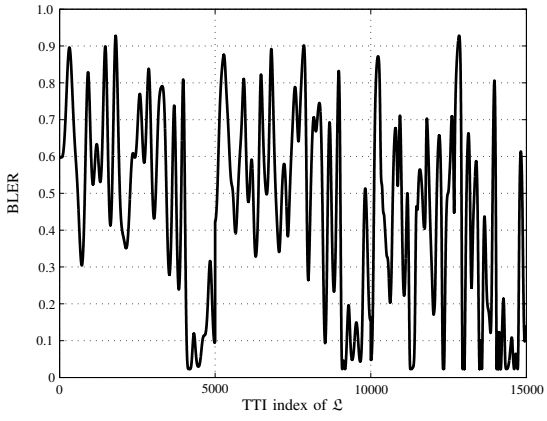

(b)

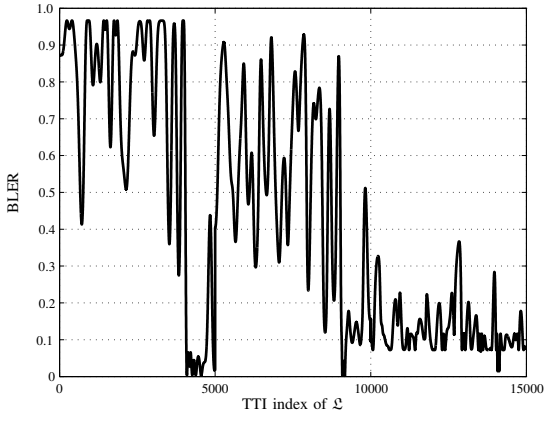

(c)

Fig. 9. Results for p prediction through (b) classical EESM and (c) extended EESM; the actual p are presented in (a).

of the weak fails is not enough to substantially deviate the link adaptation or radio resource management decisions but the strong fails are, the scenario with a lot of small square errors will be preferable.

As an example, we can set the threshold 0.16 of square

error for classifying the interfacing fails between weak and strong. Taking the whole simulation for each L2S interface, we have captured 2 310 strong fails for the classical EESM against 713 for the extended EESM. In addition, we have conducted four other simulation campaigns with independent channel realizations, but under similar conditions. The amounts of strong fail occurrences are gathered in Table II.

TABLE II
NUMBER OF STRONG FAIL OCCURRENCES FOR DIFFERENT SIMULATION CAMPAIGNS, GIVEN THE THRESHOLD OF 0.16.

campaign index	classical EESM	extended EESM
1	2 310	713
2	1 800	607
3	1 731	553
4	1 928	661
5	1 804	439

The ratio between the number of strong fail occurrences of classical and extended EESM varies significantly over the simulation campaigns. On our simulations, this ratio ranged from 2.9 to 4.1, always keeping the extended EESM as the least harmful interface option.

In Fig. 10, the histogram of square errors is disposed in intervals, from the weakest — square error in $[0.0, 0.1]$ — up to the strongest one — square error in $]0.9, 1.0]$ —, together with the confidence intervals at 90% level. Taking the mean values in each interval of square errors, the performance of interfaces can be further analyzed. The extended EESM has presented 19.65% larger number of weakest fail occurrences. Conversely, the extended EESM outperformed the classical one in all other square error significant intervals, reducing the square error occurrences in 54.34%, 55.46%, 86.84%, 91.27%, 90.66% and 100.0%, respectively for the intervals $]0.1, 0.2]$, $]0.2, 0.3]$, $]0.3, 0.4]$, $]0.4, 0.5]$, $]0.5, 0.6]$ and $]0.6, 0.7]$. Thus, extended EESM was shown to be more reliable than the classical one, specially for the highest square errors, which are the most harmful for the SLS.

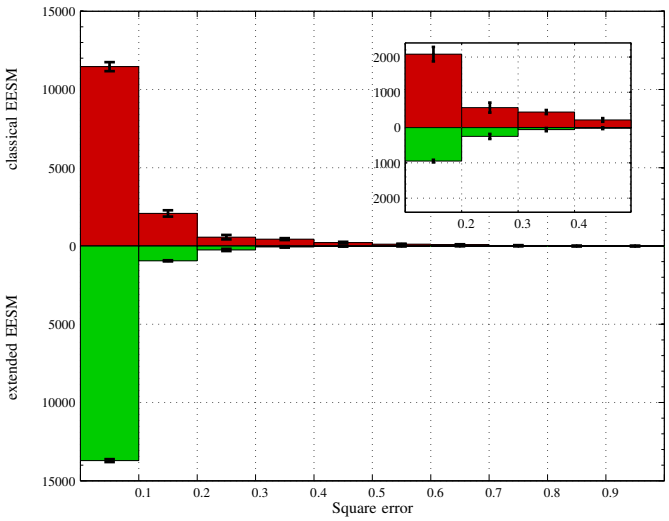

Fig. 10. Histogram of square errors provided by the classical and extended versions of EESM over five independent channel realizations. Confidence level of 90%.

VI. CONCLUSIONS

In this work we addressed a special shortcoming of exponential ESM (EESM) link-to-system level (L2S) interface: the inability to discern between participations of thermal noise and interference on the link-level behavior. The key issue to tackle the problem is to make use of information about the interference to a better tunning of EESM. We introduced the extended EESM, which, via computer simulations, showed to be able to solve that shortcoming, providing a substantial reduction of strong interfacing fail occurrences. This way, the system-level simulator (SLS) tends to be less susceptible to harmful decisions on radio resource management and link adaptation algorithms. Nevertheless, a more flexible approach must be investigated, which must be able to deal with interfere beyond discrete levels.

REFERENCES

[1] M. Dohler, R. Heath, A. Lozano, C. Papadias, and R. Valenzuela, "Is the PHY layer dead?" *Communications Magazine, IEEE*, vol. 49, no. 4, pp. 159 –165, Apr. 2011.

[2] E. M. G. Stancanelli, C. H. M. de Lima, and D. C. Moreira, *Optimizing Wireless Communication Systems*. Springer, 2009, ch. Strategies for Link-level Performance Assessment in the Simulation of Wireless Systems.

[3] H. Olofsson, M. Almgren, C. Johansson, M. Höök, and F. Kronestedt, "Improved interface between link level and system level simulations applied to GSM," *IEEE 6th International Conference on Universal Personal Communications*, vol. 1, p. 7983, Oct. 1997.

[4] H. Holma, "A study of UMTS terrestrial radio access performance," Ph.D. dissertation, Helsinki University of Technology, Espoo, Finland, Oct. 2003.

[5] K. Brueninghaus, D. Astély, T. Sälzer, S. Visuri, A. Alexiou, S. Karger, and G.-A. Seraji, "Link performance models for system level simulations of broadband radio access systems," *IEEE International Symposium on Personal, Indoor and Mobile Radio Communications*, vol. 4, pp. 2306–2311, Sept. 2005.

[6] E. Tuomaala and H. Wang, "Effective SINR approach of link to system mapping in OFDM/multi-carrier mobile network," *2nd International Conference on Mobile Technology, Applications and Systems*, vol. 2, Nov. 2005.

[7] 3rd Generation Partnership Project (3GPP). [Online]. Available: http://www.3gpp.org

[8] 3GPP, "Spatial channel model for Multiple Input Multiple Output (MIMO) simulations," 3GPP, Tech. Rep. TR 25.996 V8.0.0, Dec. 2008.

[9] ——, "Physical Layer Aspects for Evolved Universal Terrestrial Radio Access (UTRA)," 3^{rd} Generation Partnership Project, Tech. Rep. TR 25.814 V7.1.0 - Release 7, Sept. 2006. [Online]. Available: http://www.3gpp.org

[10] M. Pauli, U. Wachsmann, and S.-H. S. Tsai, "Quality determination for a wireless communications link," United States Patent Application Publication, Oct. 2004.

[11] E. Westman, "Calibration and Evaluation of the Exponential Effective SINR Mapping (EESM) in 802.16," Master's thesis, Royal Institute of Technology, Stockholm, Sweden, Sept. 2006.

[12] ITU, "Guidelines for evaluation of radio transmission technologies for IMT-2000," Tech. Rep. ITU-R Recommendation ITU-R M.1225, 1997. [Online]. Available: http://www.itu.int